Thermodynamic Characterization of the Human Acidic Fibroblast Growth Factor: Evidence for Cold Denaturation†

Ya-hui Chi,‡ Thallampuranam Krishnaswamy S. Kumar,‡ Han-Min Wang,‡ Meng-Chiao Ho,‡ Ing-Ming Chiu,§ and Chin Yu*,‡

Department of Chemistry, National Tsing Hua University, Hsinchu, Taiwan, and Department of Internal Medicine, Davis Medical Research Center, The Ohio State University, Columbus, Ohio 43210

Received October 11, 2000; Revised Manuscript Received April 2, 2001

ABSTRACT: The thermodynamic parameters characterizing the conformational stability of the human acidic fibroblast growth factor (hFGF-1) have been determined by isothermal urea denaturation and thermal denaturation at fixed concentrations of urea using fluorescence and far-UV CD circular dichroism (CD) spectroscopy. The equilibrium unfolding transitions at pH 7.0 are adequately described by a two-state (native ↔ unfolded state) mechanism. The stability of the protein is pH-dependent, and the protein unfolds completely below pH 3.0 (at 25 °C). hFGF-1 is shown to undergo a two-state transition only in a narrow pH range (pH 7.0−8.0). Under acidic (pH <6.0) and basic (pH >8.0) conditions, hFGF-1 is found to unfold noncooperatively, involving the accumulation of intermediates. The average temperature of maximum stability is determined to be 295.2 K. The heat capacity change (ΔC_p) for the unfolding of hFGF-1 is estimated to be 2.1 ± 0.5 kcal·mol^{-1}·K^{-1}. Temperature denaturation experiments in the absence and presence of urea show that hFGF-1 has a tendency to undergo cold denaturation. Two-dimensional ^{1}H−^{15}N HSQC spectra of hFGF-1 acquired at subzero temperatures clearly show that hFGF-1 unfolds under low-temperature conditions. The significance of the noncooperative unfolding under acidic conditions and the cold denaturation process observed in hFGF-1 are discussed in detail.

Human acidic fibroblast growth factor (hFGF-1) is a 16 kDa all-β-sheet protein, bereft of disulfide bonds. hFGF-1 is a powerful mitogen and plays key roles in morphogenesis, development, angiogenesis, and wound healing (*1*−*3*). hFGF-1 is known to bind to heparin and related polyanions with high affinity (*4*−*6*). Elegant in vitro studies by Middaugh and co-workers showed that heparin and other polyanionic ligands protect the protein from extremes of temperature and enzymatic proteolysis and consequently enhance its (hFGF-1) mitogenic activity (*7*, *8*).

hFGF-1 triggers mitogenic activity by binding specifically to the tryosine kinase receptors at the cell surface (*9*, *10*). It has been shown that interaction of hFGF-1 with heparin/heparan sulfate proteoglycans results in the dimerization of the growth factor molecule and consequently increases its binding affinity to the receptor. Binding of hFGF-1 (in its oligomerized state) is suggested to result in the activation of the receptor (*9*, *10*).

Membrane insertion and protein translocation are known to be mediated by a nonpolar signal peptide present upstream of the N-terminus of the protein destined to be transported to various organelles (*11*). Interestingly, hFGF-1 lacks the characteristic secretion signal sequence (*11*, *12*). Hence, it is still unknown as to how the hFGF-1 synthesized in the cytosol transports itself across the cell membrane to bind to its cell surface receptor. Wiedlocha et al. reported the translocation of hFGF-1 fused to diphtheria toxin across the cytosolic membrane strictly under acidic conditions (*13*). However, the translocation process was shown to be inhibited in the presence of sulfate polyanions, which stabilize the structure of hFGF-1. Subsequent studies showed hFGF-1 to exist in a partially structured state(s), which possess(es) high affinity to bind to negatively charged phospholipid vesicles (*7*, *8*, *14*−*16*). These studies clearly show that the modulation of the conformational stability permits hFGF-1 to traverse across the cell membrane (*15*, *16*). In this context, in the present study we describe the thermodynamics of the unfolding of hFGF-1 using a variety of biophysical techniques including multidimensional NMR methods. The results obtained herein demonstrate that hFGF-1 undergoes profound pH-dependent conformational changes and the pH-induced unfolding of the protein under acidic conditions (pH <6.0) is shown to proceed via the accumulation of intermediate(s). In addition, we also provide evidence to show that hFGF-1 exhibits a tendency to undergo cold denaturation.

MATERIALS AND METHODS

Heparin−Sepharose was obtained from Pharmacia Amersham, USA. Labeled $^{15}NH_4Cl$ were purchased from Cambridge Isotope Laboratories, USA. Ultrapure urea was purchased from Sigma Chemical Co., St. Louis, MO. All other chemicals used were of high quality analytical grade. The concentration of urea was estimated using established procedures (*17*).

† This work was supported by the National Science Council, Taiwan, and the Dr. C. S. Tsou Memorial Research Foundation.

* To whom all correspondence has to be addressed. E-mail: cyu@mx.nthu.edu.tw. Fax: 886-35-711082.

‡ National Tsing Hua University.

§ The Ohio State University.

10.1021/bi002364+ CCC: $20.00
Published on Web 05/26/2001

Protein Expression and Purification. Residues are numbered as per their position in the primary structure of the 154 amino acid hFGF-1. The expression vector for the truncated form of the human FGF-1 (hFGF-1, residues 15−154) was constructed and inserted between the *Nde*I and *Bam*H1 restriction sites in pET20b. The plasmid containing the hFGF-1 insert was transformed into *Escherichia coli* BL21 (DE3) pLysS. The expressed protein was purified on heparin−Sepharose using a NaCl gradient (0−1.5 M). The protein was desalted by ultrafiltration using an Amicon setup. The homogeneity of the protein was assessed using SDS−PAGE. The authenticity of the sample was further verified by ES−mass analysis. The concentration of the protein was estimated from the extinction coefficient value of the protein at 280 nm.

Steady-State Fluorescence Measurements. All fluorescence spectra were collected on a Hitachi F-2500 spectrofluorometer at 2.5 nm resolution, using an excitation wavelength of 280 nm. Fluorescence measurements were made at a protein concentration of 10 μg/mL. Each spectrum was an average of five scans.

pH-Induced Denaturation. The pH-induced denaturation experiments were monitored by fluorescence (Hitachi F-2500 spectrofluorometer) and far-UV CD (at 228 nm) spectroscopy (Jasco J720 spectrofluorometer) at 25 °C. Phosphate buffer was used throughout the pH range. Phosphoric acid (10 mM) was titrated with the NaOH to obtain the required pH. The pH of the prepared buffer was checked repeatedly after the addition of the protein and/or urea to ensure the accuracy of the measured pH. A maximum variation of ±0.05 pH unit was allowed in all of the buffer preparations. However, in the thermal denaturation experiments a maximum deviation of 0.1 pH unit (from the required pH) was observed.

Urea-Induced Unfolding. Urea-induced unfolding at all temperatures and pH conditions was performed using far-UV CD and fluorescence techniques. For the unfolding experiments, appropriate concentrations of urea were dissolved in 10 mM phosphate buffer (at the desired pH) containing 100 mM sodium chloride. For the thermal denaturation experiments at fixed amounts of urea, sample exposure to high temperatures was kept short to minimize any protein modification by urea decomposition products and consequent irreversibility.

Thermal Denaturation. Thermal denaturation experiments were carried out in the temperature range of 277−337 K using fluorescence and far-UV CD. For the thermal unfolding experiments, the requisite temperature was attained using a NesLab circulating water bath. Temperature-induced CD experiments were performed using a 0.1 cm water-jacketed quartz cell.

Data Analysis. The equilibrium unfolding data were analyzed using the two-state [native (N) ↔ unfolded (U) state] model of unfolding (*18*−*20*) by converting the raw data to the fraction of the protein in the unfolded state (f_u), as a function of the urea concentration using the equation

$$f_u = \{Y_I - (Y_f + m_f[D])\}/\{(Y_u + m_u[D]) - (Y_f + m_f[D])\} \quad (1)$$

where Y_I is the observed spectroscopic property, Y_f and m_f are the intercept and slope of the folded state baseline, and Y_u and m_u represent the respective intercept and slope values of the unfolded baseline. [D] is the molar denaturant concentration and

$$\Delta G_u = -RT \ln K_{eq} \quad (2)$$

where K_{eq} is the equilibrium constant, ΔG_u is the change in free energy in the presence of the denaturant, R is the gas constant, and

$$K_{eq} = f_u/f_n \quad (3)$$

where f_n is the fraction of the protein in the folded state $= 1 - f_u$.

The raw thermal denaturation data were converted to the fraction of the unfolded species (f_u) as a function of the temperature as

$$K_{eq} = f_u/(1 - f_u) = \{Y_I - (Y_f + m_f T)\}/\{(Y_u + m_u T) - Y_I\} \quad (4)$$

A two-state unfolding process is characterized by a change in heat capacity (ΔC_p) that is independent of temperature in the range of measurements (*21*, *22*). This parameter provides the temperature dependence to ΔG, ΔH (change in enthalpy), and ΔS (change in entropy)

$$\Delta G = \Delta H - T\Delta S \quad (5)$$

$$\Delta H(T) = \Delta H_m + \Delta C_p(T - T_m) \quad (6)$$

$$\Delta S(T) = \Delta S_m + \Delta C_p \ln(T/T_m) \quad (7)$$

$$\Delta G(T) = \Delta H_m\{1 - (T/T_m)\} - \Delta C_p\{(T_m - T) + T \ln(T/T_m)\} \quad (8)$$

T_m corresponds to the midpoint of the thermal transition, wherein $\Delta G(T) = 0$. ΔH_m and ΔS_m are the values of ΔH and ΔS at T_m.

According to the linear free energy model, all of the changes in $\Delta G'$, $\Delta H'$, $\Delta S'$, and $\Delta C_p'$ that occur during protein unfolding have a linear dependence on the molar concentration of denaturant, and their relationship is given by the equations

$$\Delta G' = \Delta G + m(D) \quad (9)$$

$$\Delta H' = \Delta H + h(D) \quad (10)$$

$$\Delta S' = \Delta S + s(D) \quad (11)$$

$$\Delta C_p' = \Delta C_p + c(D) \quad (12)$$

where the primes on the above parameters are the values determined in the presence of urea and m, h, s, and c are a measure of the protein−denaturant interaction.

NMR Experiments. All NMR experiments were carried out on a Bruker DMX 600 MHz spectrometer in 10 mM phosphate buffer (pH 6.5) containing 100 mM ammonium sulfate. The temperature-dependent amide proton chemical shifts in hFGF-1 were monitored from $^1H-^{15}N$ HSQC over a temperature range of 263−298 K at 5 K intervals. The probe temperature was calibrated with ethylene glycol. A 5 mm inverse probe with a self-shielded z-gradient was used to obtain all gradient-enhanced $^1H-^{15}N$ HSQC spectra. ^{15}N decoupling during acquisition was accomplished using the

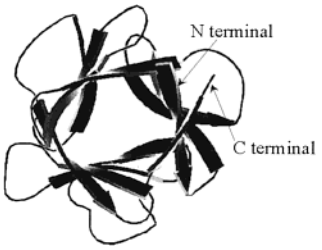

FIGURE 1: MOLSCRIPT representation of the structure of hFGF-1. The protein consists of 12 β-strands arranged antiparallelly into a β-barrel structure.

GARP sequence. A total of 2048 complex data points were collected in the ^{1}H dimension of the ^{1}H−^{15}N HSQC experiments. A modified sensitivity-enhanced gradient HSQC experiment was utilized, incorporating additional pulsed field gradients for artifact suppression (*23*, *24*). In the indirect ^{15}N dimension of the spectra, 512 complex data points were collected. The concentration of the protein sample was 1.5 mM in 100 mM phosphate buffer (in 90% H_2O and 10% D_2O) containing 100 mM ammonium sulfate. In the temperature range used for the NMR experiments the sample remained in solution without freezing. Assignments of the cross-peaks in the ^{1}H−^{15}N HSQC spectra were reported previously by Ogura et al. (*25*). ^{15}N chemical shifts were referenced using the consensus ratio of 0.010 132 911 8. All spectra were processed on a Silicon Graphics workstation using the UXNMR and Aurelia softwares.

RESULTS AND DISCUSSION

The hFGF-1 consists of 12 β-strands arranged antiparallelly into a β-barrel structure (Figure 1; *25*−*29*). The protein has a single tryptophan residue located at position 121. The fluorescence spectrum of hFGF-1 shows an emission maximum around 308 nm (*6*, *7*). The fluorescence of the lone tryptophan is completely quenched in the native state. The quenching effect is attributed to the presence of imidazole and pyrrole moieties located in the vicinity of the indole group of Trp121 in the three-dimensional structure of hFGF-1 (*6*, *7*). However, this quenching effect is relieved upon unfolding, and the fluorescence spectrum of the protein in the unfolded state shows an emission maximum around 350 nm. These spectral features are ideal to monitor the conformational changes induced in the protein during the unfolding process.

pH-Induced Unfolding. The conformational stability of hFGF-1 in the pH range of 1.0−12.0 was monitored using the emission intensity changes at 350 nm. It could be discerned from Figure 2 that the protein retains its native state in the pH range of 5.0−9.0. Beyond this pH range, the protein is observed to undergo drastic conformational changes leading to unfolding. The fluorescence spectra of the protein obtained under highly acidic (pH 3.0−1.0) and basic (pH 10−12.0) conditions are representative of the protein in the unfolded state. The small decrease in the 308 nm/350 nm emission ratio observed at either extremes of the pH range is due to the conformation-independent changes in the intrinsic tryptophan fluorescence under extremely acidic (pH <3.0) and basic conditions (pH >10.0). To ensure that changes in the Trp emission are not simply reflecting local unfolding event(s), we monitored the pH-induced conformational changes in hFGF-1 using far-UV circular

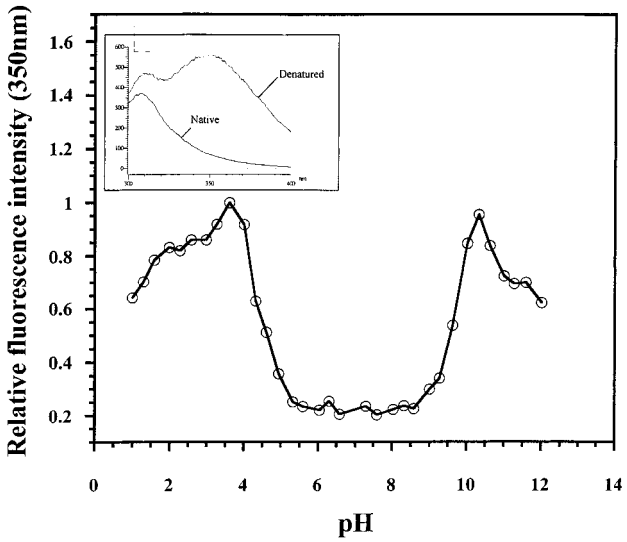

FIGURE 2: pH-induced unfolding of hFGF-1 monitored by fluorescence using the 350/308 nm ratio. The inset depicts the native and unfolded states of hFGF-1 as monitored by fluorescence.

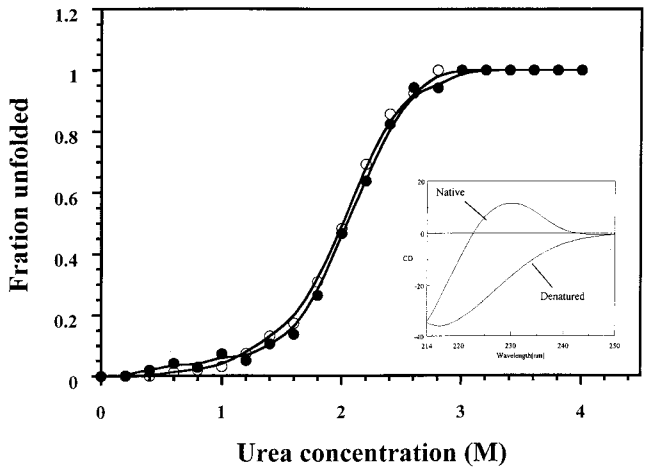

FIGURE 3: Urea-induced unfolding of hFGF-1 at pH 7.2 monitored by (○) far-UV CD (at 228 nm) and (●) fluorescence techniques. The inset shows the far-UV CD spectrum of hFGF-1 in its native and denatured states. The *x*-axis and the *y*-axis in the inset represent the wavelength of emission (nm) and the relative fluorecence intensity, respectively.

dichroism (CD). The far-UV CD spectrum of hFGF-1 shows a strong positive ellipticity band at 228 nm and an intense negative ellipticity peak at 205 nm, characteristic of type β-II proteins. The 228 nm CD band is representative of both secondary and tertiary structural interactions in the protein. In the completely unfolded state, the 228 nm CD band changes sign to yield negative ellipticity values (Figure 3, inset). These spectral characteristics are useful to probe the structural changes occurring during the unfolding of the protein. The pH-induced profile monitored by the changes in the far-UV CD ellipticity (at 228 nm) shows a trend similar to that obtained using the tryptophan fluorescence (data not shown).

Two-State Unfolding. The relative thermodynamic stability of hFGF-1 in the pH range of 4.0−9.0 was assessed on the basis of isothermal urea denaturation experiments. Figure 3 shows the equilibrium unfolding curves obtained for hFGF-1 at pH 7.0 (at 25 °C) using urea as the denaturant. The denaturation curves obtained using the fluorescence and far-UV CD spectra are nearly superimposable, indicating that

Table 1: C_m Values Estimated by Two Spectroscopic Probes

	C_m (M)			C_m (M)	
pH	far-UV CD at 228 nm	fluorescence (350/308 nm)	pH	far-UV CD at 228 nm	fluorescence (350/308 nm)
4	0.0992	0.145	7	1.978	1.978
4.5	0.375	0.387	7.5	ND	1.916
5	0.853	0.923	8	1.652	1.672
5.5	ND[a]	1.119	8.5	1.513	1.773
6	1.349	1.677	9	0.717	1.206
6.5	ND	1.482			

[a] ND: not determined.

the urea-induced unfolding of hFGF-1 (pH 7.0) is a two-state (native ↔ unfolded state) process, without the accumulation of stable intermediates (Figure 3). The free energy for unfolding in the absence of the denaturant [$\Delta G(H_2O)$] calculated from the urea-induced unfolding profiles monitored by fluorescence and CD was 4.11 ± 0.02 kcal·mol^{-1}and 4.05 ± 0.04 kcal·mol^{-1}, respectively. Similarly, the concentration of the denaturant (C_m) at which half of the protein molecules exist in the unfolded state, was calculated to be 1.97 ± 0.02 M (by both of the CD fluorescence techniques). The "*m*" value, which is the measure of the cooperativity of the unfolding reaction, was estimated to be −2.08 ± 0.06 kcal·mol^{-1} and −2.05 ± 0.05 kcal·mol^{-1}·M^{-1} for the urea-induced unfolding curves monitored by the fluorescence and far-UV CD techniques, respectively. It should be mentioned that the urea-induced unfolding process of hFGF-1 is completely reversible.

Noncooperative Unfolding. In general, a good coincidence of the equilibrium unfolding profiles as monitored by two probes is indicative of a two-state unfolding (native ↔ unfolded state) mechanism. The urea denaturation curves of hFGF-1, obtained in the pH range of 4.0− 9.0 using fluorescence and far-UV CD, show that, except for the pH between 7.0 and 8.0, the urea-induced unfolding process at all other pH conditions (within the pH range measured) does not conform to the two-state mechanism. This feature is evident from the noncoincidence of the C_m values of the unfolding process obtained using two spectroscopic techniques (CD and fluorescence). In all cases, it is found that the far-UV CD-monitored unfolding precedes fluorescence-monitored unfolding, implying the accumulation of intermediates in the urea-induced unfolding pathway. As the protein exhibits a non-two-state unfolding behavior, the ΔG_U values could not be determined, and hence the C_m value has been used as a measure of stability of the protein in the pH range of 4.0−9.0 (Table 1). The urea unfolding experiments monitored by fluorescence at various pH conditions show that the "C_m" value is maximum in the pH range of 7.0−8.0 (Figure 4). The C_m value is noticed to decrease drastically in the acidic range below pH 6.0. In fact, the C_m value is less than 0.5 M at all pH values below 5.0 (Table 1). The *m* value of the urea unfolding curves (in the pH range of 4.0−9.0) also shows a sharp decrease at pH values less than 6.0. As the *m* value is representative of the degree of cooperativity of the unfolding process, a drastic decrease in this parameter under acidic conditions (at pH 6.0) is indicative of the formation of intermediates (in the unfolding pathway).

Thermal Denaturation of hFGF-1. The thermal denaturation of hFGF-1 at various pH values in the range of 4.0−9.0 was examined using fluorescence and far-UV CD

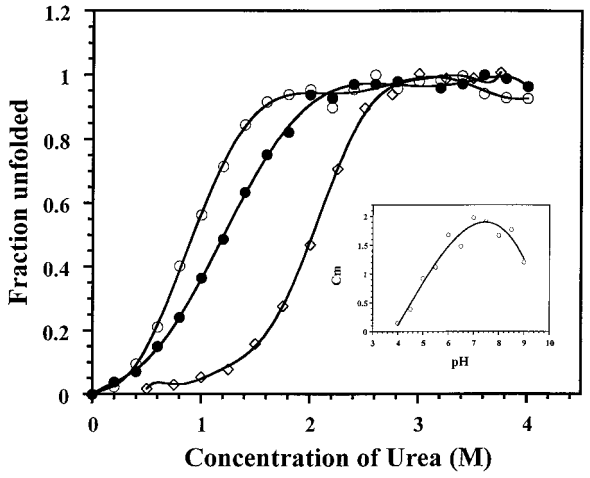

FIGURE 4: Urea denaturation curves of hFGF-1 at various pH conditions: pH 5.0 (○), pH 7.0 (◇), and pH 9.0 (●), respectively. The unfolding curves were obtained by monitoring the emission intensity changes at 350 nm. The inset depicts the change in C_m value as a function of pH. It could be noticed that the protein is maximally stable in the pH range of 7.0−8.0. The stability of the protein decreases drastically in acidic pH (pH <6.0).

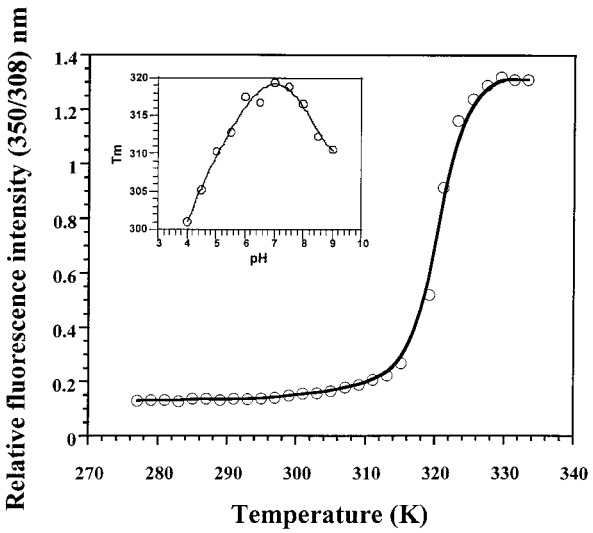

FIGURE 5: Thermal unfolding of hFGF-1 monitored by the changes in the 350 nm fluorescence. The inset shows the change in T_m as a function of pH.

spectroscopy. Temperature-induced unfolding curves monitored by these two spectroscopic techniques were only found to be cooperative in the narrow pH range of 7.0−8.0. Beyond this pH range, the thermal unfolding of hFGF-1 is found to be noncooperative, involving the accumulation of intermediates. Figure 5 depicts the thermal denaturation profile of hFGF-1 monitored using fluorescence spectroscopy. It could be deduced that the thermal stability of the protein is maximum at pH 7.2 (T_m = 47 ± 0.25 °C). The "T_m" value shows a significant decrease in both the acidic (pH <6.0) and basic (pH >8.0) regions (Figure 5). Thus, the results of the thermal unfolding experiments seem to completely corroborate with those obtained on the basis of urea-induced unfolding.

Stability Curve and Evidence of Cold Denaturation of hFGF-1. The variation of the conformational free energy of unfolding with temperature represents the stability curve of the protein (*30*). To construct a reliable curve, enthalpy change (ΔH_m), change in excess heat capacity (ΔC_p), and

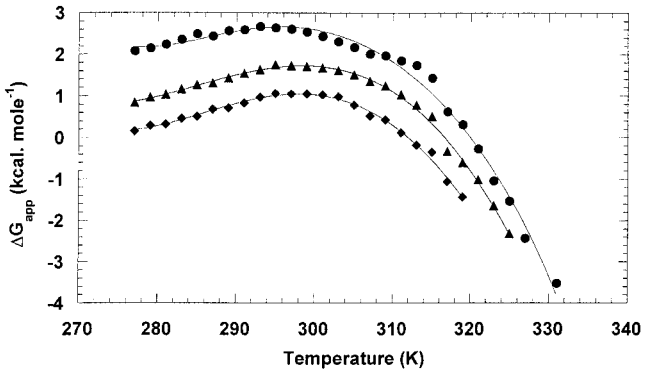

FIGURE 6: Stability curves of hFGF-1 at pH 7.0 as a function of temperature at various concentrations of urea and in the absence of the denaturant at 0 M urea (●), in 1 M urea (▲), and in 2 M urea (◆).

temperature of maximal excess heat capacity (T_m) should be known. In practice, a single thermal unfolding profile cannot provide reliable estimates of these parameters. A wider range of variability of ΔH_m and T_m could only be achieved through accurate estimation of ΔC_p by performing unfolding experiments in the presence of an additional protein stability perturbant such as urea/Gdn-HCl (*31*). In this context, we performed the thermal denaturation experiments at pH 7.2 (wherein the protein unfolds reversibly by a two-state mechanism) at 20 fixed concentrations of urea from 0 to 3.0 M in the temperature range between 277 and 337 K using fluorescence spectroscopy. Figure 6 depicts the effects of urea on the thermal stability of hFGF-1. The protein shows a tendency to undergo cold denaturation even in the absence of urea. However, in the presence of urea two unfolding transitions could be observed at high and low temperatures (Figure 6). These results suggest that hFGF-1 undergoes both cold and heat-induced denaturation.

For the thermal unfolding transitions, the apparent free energy change at any temperature in the presence and absence of urea was obtained from eqs 2−4. The temperature of maximum stability (T_s') or the temperature at which the enthalpy is zero was estimated to have an average value of 295.2 K. There is not much variation of T_s' with increasing concentration of urea (Figure 6). It should be mentioned that Schellman, using aqueous solubility of hydrocarbons as a standard representation of the hydrophobic effect, showed that the maximum temperature in the ΔG_u [in the ΔG_u versus temperature (T) plot] need not necessarily represent the temperature of maximum stability (*32*). It was suggested that the $\Delta G_u/T$ versus T plot would provide a more reliable estimate of the temperature of maximum stability of the protein (*32*). However, as only modest accuracy is attainable with the equilibrium unfolding experiments, both of the plots (ΔG_u versus T plot and the $\Delta G_u/T$ versus /T) fortuitously are expected to give the same qualitative result (data not shown). It could be seen from Figure 6 that the free energy change associated with the unfolding process decreases at both high and low temperatures. The latter is indicative of a cold denaturation process. The stability curves thus obtained were fitted to eqs 6−8 to provide estimates of ΔH_m, ΔS_m, and ΔC_p at various urea concentrations. The free energy change in hFGF-1 upon unfolding shows a strong dependence on both temperature and urea concentration. Both ΔH and ΔS show marked dependence on the denaturant concentration at all temperatures (data not shown).

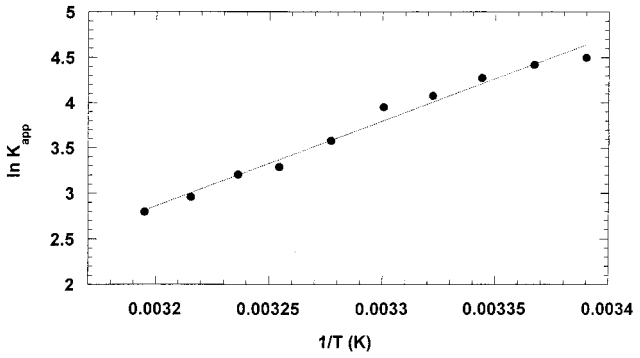

FIGURE 7: van't Hoff plot for the urea-induced unfolding of hFGF-1. The ΔH_m is estimated to be 53 ± 0.64 kcal·mol^{-1}.

Estimation of ΔC_p. The van't Hoff plot [K_{eq} versus 1/T] derived from the isothermal urea denaturation curves is shown in Figure 7. Linear least-squares fitting of the data yields a (ΔH) value of −53 ± 0.64 kcal·mol^{-1} for the urea-induced unfolding process of hFGF-1. Closer examination reveals a small curvature in the van't Hoff plot, implying that the heat capacity change (ΔC_p) has a nonzero value (*33*, *34*). In general, ΔC_p values are known to bias the slope of the van't Hoff plots producing a curvature (*33*, *35*). However, in van't Hoff data containing small ΔC_p contributions (as in the case of hFGF-1), the curvatures are known to be blurred by the noise level of the data (*33*, *36*). A nonzero ΔC_p for hGF-1 indicated by the van't Hoff data is also confirmed from the ΔH_m versus T_m plot which fits well into a straight line with a slope [$d\Delta H_m/dT_m = \Delta C_p$] of 2.1 ± 0.5 kcal·mol^{-1}·K^{-1}. The increase in ΔC_p with temperature is found to be small for hFGF-1. The ΔC_p [15.4 cal (mol of residues)$^{-1}$ K^{-1}] is found to be consistent with the average value of 14.5 cal (mol of residue)$^{-1}$ K^{-1} observed for 45 proteins in the data set of Myers et al. (*37*). ΔC_p is generally believed to be closely linked to the hydrophobic driving force and burial of nonpolar surface area. Recently, several studies have attempted to correlate the value of ΔC_p with either the total accessible area or the nonpolar surface-accessible area buried upon folding (*37*−*39*). As the total accessible area is linearly dependent on the number of residues (N_R) in the protein, Myers et al. (*37*) derived a direct relationship between C_p and "N_R" as

$$\Delta C_p = -300 + 18.6 N_R \cdot \text{cal} \cdot \text{mol}^{-1} \cdot \text{K}^{-1}$$

Estimation of the ΔC_p value of hFGF-1 (N_R = 140) based on the relationship described above yields a value of 2.3 kcal·mol^{-1}·K^{-1}. This is in close agreement with the experimentally derived value of ΔC_p (2.1 ± 0.5 kcal·mol^{-1}·K^{-1}).

Chen and Schellman recently described a procedure wherein the free energy of the stabilization curve fits a constant ΔC_p model over the entire range (*40*). This method permits an unusually complete determination of the thermodynamic parameters of the protein, and the low-temperature unfolded forms of the protein could be interpreted as an extrapolation with constant ΔC_p of the high-temperature unfolded form. Fitting to the thermal denaturation data according to the Chen and Schellman equation (*40*) yields two T_m values for the cold and hot denaturation transitions (261 ± 0.2 and 320 ± 0.6 K, respectively). These results suggest that hFGF-1 has a strong tendency to undergo cold denaturation.

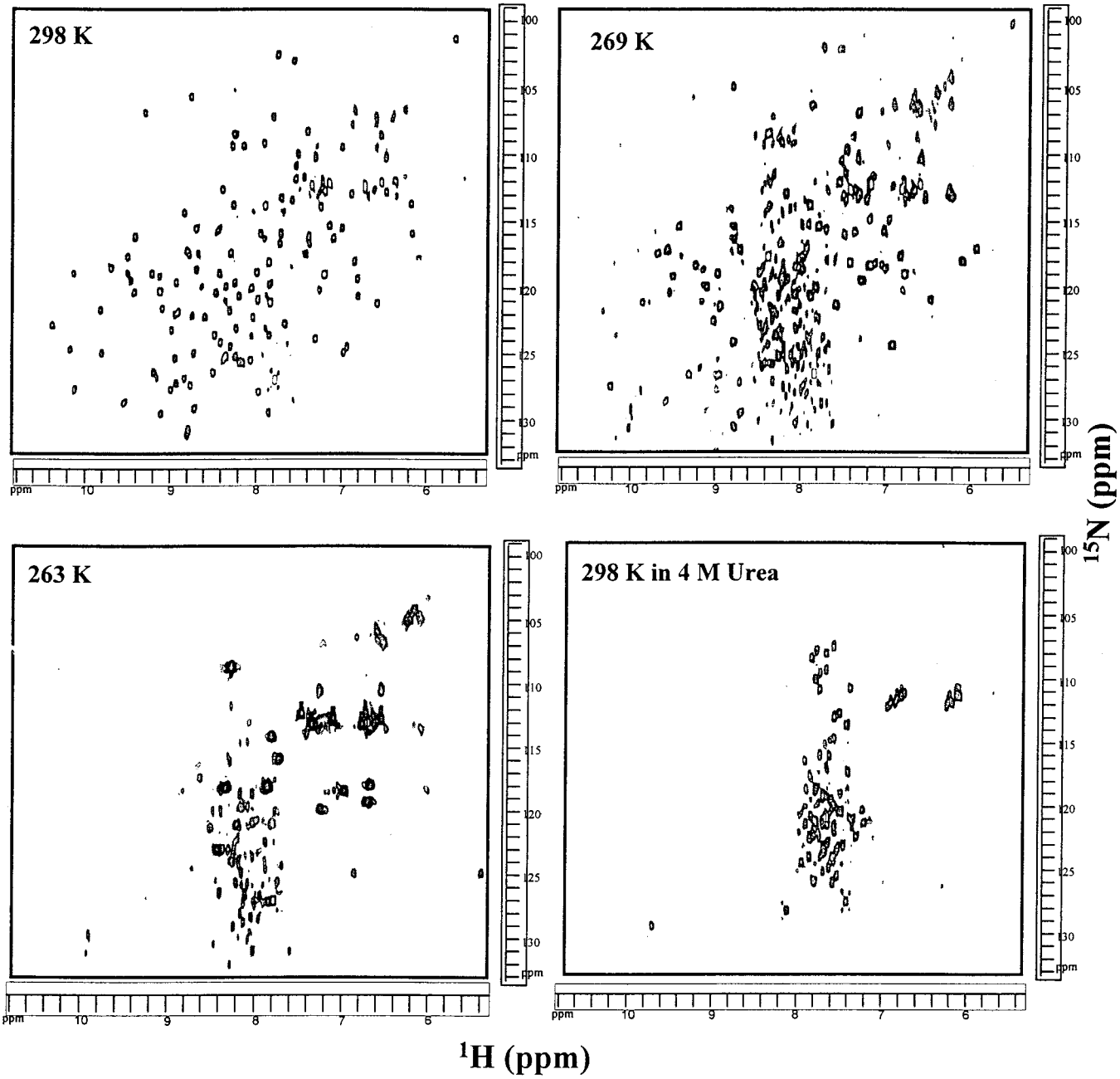

FIGURE 8: ^{1}H−^{15}N HSQC spectra of hFGF-1 at various temperatures. The spectrum at 269 K appears to represent a mixture of the native and unfolded states of the protein. The spectrum in 4 M urea represents the completely unfolded state of hFGF-1. The cross-peaks with higher intensity and chemical shift dispersion in the spectrum obtained at 263 K probably represent the residual structure in the cold denatured state of hFGF-1.

hFGF-1 exhibits several thermodynamic features which are consistent for a protein showing a tendency to undergo cold denaturation (*31*). First, the temperature of maximum stability of hFGF-1 is well above 0 °C; second, the hFGF-1 exhibits a modest maximum conformational stability (ΔG_U); finally, and most importantly, hFGF-1 shows a small $\Delta H_m/\Delta C_p$ value. The ΔC_p of hFGF-1 [15 cal (mol of residue)$^{-1}$ K^{-1}] is in the same range as the proteins [such as myoglobin (*41*), barstar (*42*), and repressor monomer (*43*)] which undergo cold denaturation. Similarly, hFGF-1 also shows a small ΔH value (27 ± 0.76 kcal·mol^{-1}). In general, the cold denaturation observed in hFGF-1 could be attributed to the weakening of the hydrophobic interactions with decreasing temperature.

NMR Evidence for Cold Denaturation. Nuclear magnetic resonance (NMR) is a powerful tool to monitor structural interactions during protein folding/unfolding (*44*, *45*). Multidimensional NMR techniques have been successfully used to structurally characterize equilibrium intermediate(s) and unfolded states of proteins (*46*, *47*). ^{1}H−^{15}N HSQC spectra were acquired at temperatures ranging from 263 to 298 K to further confirm the cold denaturation of hFGF-1 inferred from the equilibrium unfolding data obtained using optical spectroscopy (Figure 8). The ^{1}H−^{15}N HSQC spectrum of the protein at 298 K is well dispersed and is characteristic of the native state of the protein, and all of the 135 residues (leaving 5 proline residues) could be unambiguously assigned (*25*). Although the HSQC spectrum collected at 283 K shows

a strong resemblance to the one acquired at 298 K, the chemical shift dispersion (of some of the resonances) is significantly reduced. Further decrease in temperature to 269 K results in prominent crowding of many of the cross-peaks to a narrow region of the $^{1}H-^{15}N$ HSQC spectrum (Figure 8). The spectrum collected at 269 K possibly represents a mixture of native and unfolded states of the protein. Interestingly, comparison of the $^{1}H-^{15}N$ HSQC spectrum of hFGF-1 in its completely unfolded state in 4 M urea and the one collected at 263 K bears good similarity (Figure 8). The $^{1}H-^{15}N$ HSQC spectrum obtained at 263 K presents many features resembling that of an unfolded state. However, the higher intensity and chemical shift dispersion of some cross-peaks in the HSQC spectra acquired at 263 K are higher as compared to the spectrum representing the completely unfolded state in 4 M urea (Figure 8). These spectral features are reminiscent of the existence of residual structure(s) in the cold denatured state of the protein. In this context, it is interesting to note that the $^{1}H-^{15}N$ HSQC spectrum collected at 263K in 0.5 M urea closely resembles that of the completely unfolded state in 4 M urea in 298 K, suggesting the possibility of hFGF-1 existing in a partially structured state at 263 K. If true, the unfolding of hFGF-1 represents a strange case wherein the heat-induced unfolding is cooperative but the cold denaturation proceeds via the accumulation of intermediates. However, more elaborate NMR experiments need to be performed to conclusively demonstrate the existence of residual structure(s) in the cold denatured state of hFGF-1.

Relevance of the pH-Induced Intermediate State(s). The results of the present study clearly demonstrate that hFGF-1 undergoes pH-dependent conformational changes. The equilibrium unfolding experiments show that hFGF-1 reversibly unfolds by a two-state (native ↔ unfolded state) mechanism only in the narrow range of pH (pH 7.0−8.0). At acidic pH (pH <6.0), the unfolding of the protein is found to proceed via the accumulation of stable intermediates. The stable intermediate(s) under acidic conditions could be of physiological importance. hFGF-1, which lacks a translocating signal sequence to transport itself across the cell membrane (to reach its cell surface receptor), probably adopts a partially structured state to traverse across the cell membrane. The microenvironment in the vicinity of the biomembranes is contemplated to be highly acidic (*48*, *49*). In this background, it is possible that hFGF-1 synthesized on the ribosome, upon reaching the membrane, partially unfolds and exposes the buried hydrophobic sites to the solvent. The solvent-exposed nonpolar surface (in the partially structured state) is expected to provide a thermodynamically favored environment to the protein to move across the biomembrane. Upon reaching the cell surface, the proteoglycans (like heparin/heparan sulfate) on the cell membrane possibly aid the protein (hFGF-1) to regain its native structure and consequently facilitate binding to its receptor. The mechanism proposed herein for the translocation of hFGF-1 involving partially structured state(s) seems to bear relevance to the existing literature on the transport of proteins across membranes. It has been shown that molten globule-like states and/or other non-native states of protein molecules are involved in protein translocation across biomembranes (*50*−*52*).

Significance of Cold Denaturation of hFGF-1. hFGF-1 has been unambiguously shown to undergo cold denaturation at temperatures lower than 263 K. Although many proteins have been shown to undergo denaturation at low temperatures, to our knowledge there are only a few reports wherein proteins belonging to the structural class of all-β-sheet proteins have been shown to undergo cold denaturation (*53*). This study opens new avenues to understand protein folding mechanisms in hFGF-1. Characterization of the residual structures and molecular dynamics in the cold denatured state(s) of hFGF-1 would provide strong clues on the initiation sites for the refolding of the protein. In addition, as the cold denaturation process in hFGF-1 is completely reversible, the folding events on the nano- to microsecond time scale could be studied by employing the laser-induced temperature jump experiments.

Detailed structural characterization of the cold denatured state and of the pH-induced intermediate of hFGF-1 is underway in this laboratory. Results of these studies are expected to provide useful information on the relationship between folding and function of hFGF-1.

ACKNOWLEDGMENT

We thank the anonymous reviewers for their useful comments on an earlier revision of the manuscript.

REFERENCES

1. Burgess, W. H., and Maciag, T. (1989) *Annu. Rev. Biochem. 58*, 573−606.
2. Gimenez-Gallego, G., and Cuevas, P. (1994) *Neural. Res. 16*, 313−316.
3. Patrie, K. M., Botelho, M. J., Ray, S. K., Mehta, V. B., and Chiu, I. M. (1997) *Growth Factors 14*, 39−57.
4. Burke, C. J., Volkin, D. B., Mach, H., and Middaugh, C. R. (1993) *Biochemistry 32*, 6419−6426.
5. Chi, Y. H., Kumar, T. K. S., Chiu, I. M., and Yu, C. (2000) *J. Biol. Chem. 275*, 39444−39450.
6. Mach, H., Ryan, J. A., Burker, C. J., Volkin, D. B., and Middaugh, C. R. (1993) *Biochemistry 32*, 7703−7711.
7. Mach, H., and Middaugh, C. R. (1995) *Biochemistry 34*, 9913−9920.
8. Dabora, J. M., Sanyal, G., and Middaugh, C. R. (1991) *J. Biol. Chem. 266*, 23637−23640.
9. Plotnikov, A. N., Hubbard, S. R., Schlessinger, J., and Mohammadi, M. (2000) *Cell 101*, 413−426.
10. Plotnikov, A. N., Schlessinger, J., Hubbard, S. R., and Mohammadi, M. (1999) *Cell 98*, 641−650.
11. Abraham, J. A., Mergia, A., Whang, J. L., Tumolo, A., Friedman, J., Hjerrild, K. A., Gaspodarowicz, D., and Fiddes, J. C. (1986) *Science 233*, 545−548.
12. Jaye, M., Jowk, R., Burgess, W., Ricca, G. A., Chiu, I. M., Ravera, M. W., O'Brien, S. J., Modi, A. S., Maciag, T., and Drohan, W. J. (1986) *Science 233*, 541−545.
13. Wiedlocha, A., Madshus, I. H., Mach, H., Middaugh, C. R., and Olsnes, S. (1992) *EMBO. J. 11*, 4835−4842.
14. Samuel, D., Kumar, T. K. S., Srimathi, T., Hsieh, H. C., and Yu, C. (2000) *J. Biol. Chem. 275*, 34968−34975.
15. Blaber, S. I., Culajay, J. F., Khurana, A., and Blaber, M. (1999) *Biophys. J. 77*, 470−477.
16. Sanz, J. M., and Gimenez-Gallego, G. (1997) *Eur. J. Biochem. 246*, 328−335.
17. Pace, C. N. (1986) *Methods Enzymol. 131*, 266−288.
18. Santoro, M. M., and Bolen, D. W. (1992) *Biochemistry 31*, 4901−4907.
19. Schellman, J. A. (1978) *Biopolymers 7*, 1305−1322.
20. Tanford, C. (1970) *Adv. Protein Chem. 21*, 1−95.
21. Pace, C. N., Grimsely, G. R., Thomas, S. T., and Makhadatze, G. I. (1999) *Protein Sci. 8*, 1500−1504.
22. Schellman, J. A. (1987) *Annu. Rev. Biophys. Biochem. 16*, 115−137.

23. Kay, L. E., Keifer, P., and Saarinen, T. (1992) *J. Am. Chem. Soc. 114*, 10663−10664.
24. Zhang, O., and Forman-Kay, J. D. (1995) *Biochemistry 34*, 6784−6794.
25. Ogura, K., Nagata, K., Hatanaka, H., Habuchi, H., Kimata, K., Tati, S., Raveru, M. W., Jaye, M., Schlessinger, J., and Inagaki, F. (1999) *J. Biomol. NMR 13*, 11−24.
26. Pineda-Lucena, A., Jimenez, M. A., Lozano, R. M., Nieto, J. L., Santoro, J., Rico, M., and Gimenez-Gallego, G. (1996) *J. Mol. Biol. 264*, 162−178.
27. Zhu, X., Komiya, H., Chirino, A., Faham, S., Fox, G. M. Arakawa, T., Hsu, B., and Rees, D. C. (1991) *Science 251*, 90−93.
28. Zhu, X., Hsu, B. T., and Rees, D. C. (1993) *Structure 1*, 27−34.
29. Samuel, D., Kumar, T. K. S., Balamurugan, K., Lin, W. Y., Chin, D. H., and Yu, C. (2000) *J. Biol. Chem.* (in press).
30. Pace, C. N., and Laurents, D. V. (1989) *Biochemistry 28*, 2520−2525.
31. Nicholson, E. M., and Scholtz, J. M. (1996) *Biochemistry 35*, 11369−11378.
32. Schellman, J. A. (1997) *Biophys. J. 73*, 2960−2964.
33. Chaires, J. B. (1997) *Biophys. Chem. 64*, 15−23.
34. Koblan, K. S., and Ackers, G. K. (1992*) Biochemistry 31*, 57−65.
35. Liu, Y., and Sturtevent, J. M. (1997) *Biophys. Chem. 64*, 121−126.
36. Weber, G. (1996) *J. Phys. Chem. 99*, 1052−1059.
37. Myers, J. K., Pace, C. N., and Scholtz, J. M. (1995) *Protein Sci. 4*, 2138−2148.
38. Gomez, J., Hisler, V. J., Xie, D., and Freire, E. (1995) *Proteins: Struct., Funct., Genet. 22*, 404−412.
39. Khechinashvili, N. N., Janin, J., and Rodier, F. (1995) *Protein Sci. 4*, 1315−1342.
40. Chen, B., and Schellman, J. A. (1989) *Biochemistry 28*, 685−691.
41. Privalov, P. L., Griko, Y. V., Venyaminov, S. Y., and Kutyshenko, V. P. (1986) *J. Mol. Biol. 190*, 487−498.
42. Agashe, V. R., and Udgaonkar, J. B. (1995) *Biochemistry 34*, 3286−3299.
43. Huang, G. S., and Oas, T. G. (1996) *Biochemistry 35*, 6173−6180.
44. Logan, T. M., Theriault, Y., and Fesik, S. W. (1994) *J. Mol. Biol. 236*, 637−648.
45. Arcus, V. L., Vuilleumier, S., Freund, S. M. V., Bycroft, M., and Fersht, A. R. (1995) *J. Mol. Biol. 254*, 305−321.
46. Zhang, O., and Forman-Kay, J. D. (1995) *Biochemistry 34*, 3959−3970.
47. Kortemme, T., Kelly, M. J. S., Kay, L. E., Forman-Kay, J., and Serrano, L. (2000) *J. Mol. Biol. 297*, 1217−1229.
48. Endo, T., and Schatz, G. (1988) *EMBO J. 7*, 1153−1158.
49. Bychkova, V. E., Bartoshevich, S. F., and Klenin, S. I. (1990) *Biofizika (Moscow) 35*, 242−248.
50. VanderGoot, F. G., Gonzales-Manas, J. M., Lakey, J. H., and Pattus, F. (1991) *Nature 354*, 408−410.
51. VanderGoot, F. G., Lakey, J. H., and Pattus, F. (1992) *Trends Cell Biol. 2*, 343−348.
52. Bychkova, V. E., and Ptitsyn, O. B. (1993) *Chemtracts: Biochem. Mol. Biol. 4*, 133−163.
53. Pace, C. N., and Tanford, C. (1968) *Biochemistry 7*, 198−200.

BI002364+